https://doi.org/10.5194/egusphere-2025-1350
Preprint. Discussion started: 15 April 2025

NO_2 concentration differences under clear versus cloudy skies and implications for applications of satellite measurements

Daniel L. Goldberg[*,1], M. Omar Nawaz[1], Congmeng Lyu[2,3], Jian He[2,3], Annmarie G. Carlton[4], Shobha Kondragunta[5], Susan C. Anenberg[1]

[1]Department of Environmental and Occupational Health, Milken Institute School of Public Health, George Washington University, Washington, DC, USA

[2]Cooperative Institute for Research in Environmental Sciences, University of Colorado, Boulder, CO, USA

[3]NOAA Chemical Sciences Laboratory, Boulder, CO, USA

[4]Department of Chemistry, University of California - Irvine, Irvine, CA, USA

[5]NOAA NESDIS Center for Satellite Applications and Research, College Park, MD, USA

Correspondence to: Daniel L. Goldberg (dgoldberg@gwu.edu)

Abstract

Satellite measurements of tropospheric trace gases are often only used when there are few clouds, which screens out 20 – 70% of the data, depending on geographic region. While the lack of high-quality column measurements during cloudy conditions precludes validation of the satellite data, *in situ* surface measurements and model simulations can provide insight on the quantitative understanding of NO_2 during cloudy conditions. Here, we intercompare surface observations, satellite measurements, and models during 2019 over the contiguous U.S. to quantify how NO_2 concentrations are different under clear and cloudy skies. We find that *in situ* surface NO_2 measurements are, on average, +17% larger on all days compared to restricting to clear sky days and +36% larger during cloudy days versus clear sky days, with a wide distribution based on geographic region and roadway proximity: largest in the Northeast U.S. and smallest in the Southwest U.S. and near major roadways. WRF-Chem simulated surface NO_2 between cloudy and clear conditions is on average much larger than the observed differences: +59% on cloudy days vs. clear days for the model. This suggests that NO_2 in WRF-Chem is more responsive to sunlight and associated photochemistry than in reality. Finally, using *in situ* NO_2 matched to provisional TEMPO data, we find the NO_2 differences between cloudy and clear conditions to be larger in the afternoon than morning. This study quantifies some of the biases in satellite measurements introduced by using only clear-sky data, and introduces some corrections to account for these biases.

https://doi.org/10.5194/egusphere-2025-1350
Preprint. Discussion started: 15 April 2025

1 Introduction

Nitrogen dioxide (NO_2) is an air pollutant that adversely affects the human respiratory system (Health Effects Institute, 2022; Khreis et al., 2017) and can lead to premature mortality (Burnett et al., 2004; M. Z. He et al., 2020). NO_2 is also an important precursor for ozone (O_3) and fine particulates ($PM_{2.5}$), which also have serious health impacts. In urban areas, the majority of ambient NO_2 originates from local NOx emissions (=NO+NO_2; most NOx is emitted as NO which rapidly cycles to NO_2) during high-temperature fossil fuel combustion (Crippa et al., 2021). Although end-of-pipe controls (Busca et al., 1998; Koltsakis & Stamatelos, 1997) can reduce the amount of NOx emitted from engines and boilers, these technologies do not recover 100% of the NOx generation during combustion. As a consequence, NO_2 accumulates in our atmosphere and many urban areas have NO_2 concentrations that exceed the World Health Organization guideline of 5.3 ppb for an annual average (Anenberg et al., 2022).

Observing local air pollution is typically done by *in situ* surface monitors, which are spaced throughout a region with a higher density of monitors typically in areas of high population density and known pollution sources. In the United States, there are 1012 *in situ* monitoring sites measuring some combination of O_3, $PM_{2.5}$, NO_2, volatile organic compounds (VOCs), and CO (https://www.epa.gov/aqs). While the U.S. monitoring network is more comprehensive than most other countries (Martin et al., 2019), 79% of U.S. counties lack a single monitor and an additional 10% of counties have only a single monitor, leaving only 11% of U.S. counties with more than 1 monitor (Sullivan & Krupnick, 2018). Although a robust and accurate ground-monitoring network is needed, the high operating cost of these instruments can be an important barrier (Kelly et al., 2017). Spatial gaps remain in-between the regulatory monitors, and sometimes these monitors are inadequate for understanding the true ambient air pollution exposure of most U.S. residents, especially those that live and/or work several miles away from a regulatory monitor. Satellite data provide a way to fill in the gaps of the *in situ* monitoring network. Methodologies to obtain robust surface air pollutant measurement data from satellite instruments have improved dramatically in the past ten years (Bechle et al., 2015; Larkin et al., 2023; Nawaz et al., 2025; Shetty et al., 2024; W. Sun et al., 2024).

NO_2 can be observed by remote sensing instruments due to its unique spectroscopic features (Vandaele et al., 1998). The Tropospheric Monitoring Instrument (TROPOMI) (Veefkind et al., 2012) has been measuring column amounts of NO_2 pollution at ~5.5 × 3.5 km^2 spatial resolution (van Geffen, 2016) since 30 April 2018. Because of TROPOMI's higher spatial resolution over predecessor instruments, such as the Ozone Monitoring Instrument (OMI) (24 × 13 km^2 at nadir) (Levelt et al., 2018), TROPOMI has ~50 daily satellite pixel measurements within a typical city (~1000 km^2) during clear skies, while OMI may have only 1-3 daily measurements within the borders of each city. This increased measurement capacity within a city allows us to discern spatial variability undetectable by previous instruments. Further, the data from the satellite instruments can be downscaled using a process called oversampling (de Foy et al., 2009; K. Sun et al., 2018), which re-grids the irregular satellite pixels to a standard and higher spatial resolution. The spatial resolution is thus effectively increased at the expense of the temporal resolution.

NO_2 satellite measurements are of the tropospheric column. In many cases, NO_2 column measurements are strongly correlated with the spatial patterns of surface NO_2 concentrations (Acker et al., 2025; Harkey & Holloway, 2024; Kim

https://doi.org/10.5194/egusphere-2025-1350
Preprint. Discussion started: 15 April 2025

et al., 2024) and surface NOx emissions (Goldberg et al., 2024). For TROPOMI, studies have shown a strong correlation between tropospheric column measurements and collocated surface NO_2 for both the 13:30 average (r^2 = 0.67) and the 24-hour average (r^2 = 0.68) (Goldberg et al., 2021; Kerr et al., 2023). However, there are rare instances in which NOx emissions and NO_2 enhancements stay aloft and do not affect the surface; these are often situations associated with lightning NOx (Nault et al., 2017), wildfire NOx (Jin et al., 2021; Lin et al., 2024), and aircraft NOx (Maruhashi et al., 2024). In these instances, it can be difficult to determine if the column NO_2 enhancements are also leading to surface NO_2 enhancements. These misinterpretations are more likely to occur over rural regions and/or individual days, as upper-tropospheric NO_2 enhancements near urban regions often dwarf NO_2 enhancements within the boundary layer especially over monthly or longer timescales (Goldberg et al., 2022).

Satellite measurements of trace gases are typically only used when there are few or no clouds; this is often referred to as the clear-sky bias of satellite data. This results in 20 – 70% of the satellite data being filtered out depending on geographic region. The clear-sky bias affects NO_2 moreso than other trace gases (such as CO and CH_4) because NO_2 is very photochemically active in the presence of strong sunlight; its effective lifetime during summer daytime is 2 – 7 hours (F. Liu et al., 2016) and conversely can be up to 30 hours during winter daytime (Kenagy et al., 2018). The speed at which it transforms into other chemical species is determined by the strength of sunlight, ambient temperature, and oxidation environment (Laughner & Cohen, 2019; Shah et al., 2020). More specifically, NO_2 can react with OH to create HNO_3 (which is usually considered a terminal sink), NO_2 can photolyze and facilitate the formation of O_3 in the presence of volatile organic compounds, and NO_2 can react with VOCs to create organic nitrates (e.g., peroxyacetyl nitrates and alkyl nitrates) (Zare et al., 2018) with the latter two being temporary sinks of NO_2. Another daytime terminal sink for NO_2 is dry deposition; while this removal mechanism is often secondary to photochemical loss in urban environments and is not directly affected by sunlight, it is indirectly affected as cloudy conditions are often associated with increased relative humidity and shallower boundary layer depths, both of which increase dry deposition. Therefore, increased NO_2 dry deposition in cloudy conditions could offset some of the decreased NO_2 photochemical loss rates. The net result is that NO_2 concentrations are typically larger during cloudy conditions (Geddes et al., 2012).

However, outside of the Geddes et al. (2012) study, little has been done to observationally quantify the bias of NO_2 being larger during cloudy conditions particularly because there are no column measurements to validate the satellite during cloudy conditions. With that said, there are surface *in situ* measurements during cloudy conditions that can give us an idea of how the clear-sky bias may affect the estimate of surface concentrations. In this project, we intercompare surface observations, satellite measurements, and models under clear and cloudy skies to better quantify the amount of surface bias of NO_2 concentrations that is being introduced when clouds are screened from the satellite data. Our analysis is focused on the United States during 2019 due the high density of *in situ* monitors and availability of high-resolution regional chemical transport models. The motivation of this project is two-fold: 1) to determine what the scientific community may be missing when excluding clouds from satellite-based NO_2 analyses and 2) to understand how geostationary NO_2 satellite measurements may be affected by such a bias and potentially partially remediate such a bias.

https://doi.org/10.5194/egusphere-2025-1350
Preprint. Discussion started: 15 April 2025

2 Methods

2.1 EPA AQS Data

Hourly *in situ* NO_2 measurements were obtained from the pre-generated EPA Air Quality System (AQS) database: https://aqs.epa.gov/aqsweb/airdata/download_files.html. These routine measurements are operated and maintained by various state and federal agencies. 91% of the "NO_2" measurements in 2019 were acquired through a chemiluminescence technique which converts NO_2 and a small amount of NO_y species – such as alkyl nitrates, peroxynitrates, and nitric acid – to NO using a heated molybdenum converter, and the NO is measured by quantifying the luminesce of NO when reacted in excess O_3 (Dickerson et al., 2019). Other methods to measure *in situ* NO_2 include Cavity Attenuated Phase Shift (Kebabian et al., 2008) and Laser Induced Fluorescence (Thornton et al., 2000), but these methods are less common (9% of all NO_2 monitors in 2019) and more expensive to operate and maintain. Annual and seasonal averages at 13:30 local standard time (between 13:00 – 14:00) of the *in situ* data were considered valid and used if more than 75% of the days of the year/season had valid data. There were 449 monitoring locations in 2019 in the U.S. that achieved these criteria for an annual average, which equates to 1 monitor per ~730,000 U.S. residents. For the baseline analysis, we further remove data from the 75 monitoring locations (17% of the locations) that are classified as "near-road" by the EPA, which means that they are installed within 20 m from major interstates since these *in situ* measurements are not representative of a ~20 km^2 satellite pixel measurement; we include the "near-road" NO_2 monitoring data in sensitivity analyses. NO_2 measurements between cloudy and clear-sky days are intercompared using the normalized mean change (NMC) as described in Equation 1, where $\bar{x}$ and $\bar{y}$ are means of the two datasets being analyzed.

$$NMC(\%) = 100 \times \left(\frac{\bar{y}-\bar{x}}{\bar{x}}\right) \quad (1)$$

2.2 Satellite NO_2 Instruments

NO_2 slant column densities are derived from radiance measurements in the 405 – 465 nm spectral window of the UV-VIS-NIR spectrometer (van Geffen et al., 2021). Satellite instruments observe NO_2 by comparing observed spectra with a reference spectrum to derive the amount of NO_2 in the atmosphere between the instrument and the surface; this technique is called differential optical absorption spectroscopy (DOAS) (Platt, 1994). Tropospheric vertical column density data, which represent the vertically integrated number of NO_2 molecules per unit area between the surface and the tropopause, are then calculated by subtracting the stratospheric portion and then converting the tropospheric slant column to a vertical column using an air mass factor (AMF) (Boersma et al., 2011). The AMF is a unitless quantity used to convert the slant column into a vertical column and is a function of the satellite viewing angles, solar angles,

https://doi.org/10.5194/egusphere-2025-1350
Preprint. Discussion started: 15 April 2025

the effective cloud radiance fraction and pressure, the vertical profile shape of NO_2 provided by a chemical transport model simulation, and the surface reflectivity (Lorente et al., 2017; Palmer et al., 2001).

2.2.1 TROPOMI

TROPOMI was launched by the European Space Agency (ESA) on 13 October 2017, and data from the instrument became available on 30 April 2018, after an approximately 6-month calibration period. The satellite follows a sun-synchronous, low-earth (825 km) orbit with an equator overpass time of approximately 13:30 local solar time. TROPOMI measures total column amounts of several trace gases: NO_2, HCHO, O_3, CO, CH_4, among others. At nadir, pixel sizes are 3.5×7 km^2 (modified to 3.5×5.5 km^2 on August 6, 2019) with the edges having slightly larger pixels sizes (~14 km wide) across a 2600 km swath, equating to 450 rows (van Geffen et al., 2020).

For our analysis we use the TROPOMI NO_2 version 2.4 (v2.4) re-processed algorithm during Jan 1, 2019 – Dec 31, 2019. The TROPOMI NO_2 v2.4 product has a documented median low bias of -34.8% in moderately polluted locations (when NO_2 measurements are between 3 – 14 x 10^{15} molec/cm^2) when compared to a MAX-DOAS network (Lambert et al., 2023). Prior work has demonstrated a strong correlation between TROPOMI NO_2 column measurements and NO_2 surface concentrations in urban areas (Demetillo et al., 2020; Dressel et al., 2022; Goldberg et al., 2021; Nawaz et al., 2025). For our baseline, we screened TROPOMI pixels for quality assurance flag values greater than 0.75, and conduct a sensitivity analysis of filtering only with a cloud radiative fraction filter of 0.5. The cloud radiative fraction is calculated from the O_2 A-band using the FRESCO-S algorithm. Due to differences in wavelength between the O_2 A-band and the NO_2 retrieval window, the cloud fraction retrieved in the O_2 A-band is not exactly representative for the cloud fraction in the NO_2 window, but it is similar.

The filtered data were re-gridded to a $0.01° \times 0.01°$ resolution, to create a custom "Level-3" data product (Goldberg et al., 2021) during cloud-free and cloudy conditions. Single pixel TROPOMI tropospheric vertical column NO_2 uncertainties have been quantified to be between 25 – 50% under clear skies and this uncertainty is dominated by uncertainty in the tropospheric air mass factor (Glissenaar et al., 2025; S. Liu et al., 2021; Rijsdijk et al., 2025); uncertainties of measurements with cloud fractions > 0.5 are larger. Oversampled NO_2 measurements over monthly and annual timeframes (10s - 100s of measurements) have a smaller amount of uncertainty, approximately 10 – 20 % depending on location and season (Glissenaar et al., 2025) .

2.2.2 TEMPO

TEMPO was launched by SpaceX on 7 April 2023 and is hosted on Maxar Intelsat 40e. Data from the instrument became available on 2 August 2023, after an approximately 4-month dry-out, cool-down, and calibration period. The satellite is in geostationary orbit centered over the United States with north-south coverage extending from Mexico to southern Canada and east-west coverage from Puerto Rico to the Pacific coast. TEMPO operationally measures total column amounts of NO_2, HCHO, and O_3 with additional products forthcoming. At nadir, pixel sizes are 4.75×2 km^2

https://doi.org/10.5194/egusphere-2025-1350
Preprint. Discussion started: 15 April 2025

with the North-east and North-west edges having slightly larger pixels sizes. The instrument observes the full east-west swath approximately once every hour.

For our analysis we use the TEMPO NO_2 version 3 algorithm during 2 Aug 2023 – 31 Aug 2024. The data was filtered to include pixels only where the effective cloud fractions are less than 0.15 and the main data quality flags are equal to 0. The filtered data was re-gridded to a 0.01° × 0.01° resolution, to create a custom "Level-3" data product (Goldberg et al., 2021) during cloud-free and cloudy conditions. Single pixel TEMPO tropospheric vertical column NO_2 uncertainties can be assumed to be similar to the uncertainty of TROPOMI measurements (Glissenaar et al., 2025), which are between 25 – 50% under clear skies for individual pixels, and 10 – 20% for oversampled averages; future work will better quantify the uncertainties of TEMPO NO_2 measurements.

2.3 ERA5 Re-analysis

We intercompare the cloud radiative fractions from TROPOMI to the ERA5 re-analysis (Hersbach et al., 2020) of total cloud fractions in the early afternoon (18Z for Eastern Time, 19Z for Central Time, 20Z for Mountain Time, 21Z for Pacific Time), which approximates the overpass time of TROPOMI over the contiguous United States. The ERA5 total cloud fraction is a unitless quantity representing how much of a grid cell is covered by a cloud (e.g., condensed water vapor) at any vertical level of the atmosphere and does not differentiate between the optical properties of those clouds. The ERA5 re-analysis data are reported at a 0.25° × 0.25° spatial resolution and the cloud fractions are interpolated, using bilinear interpolation, to the 0.01° × 0.01° oversampled TROPOMI NO_2 grid.

2.4 WRF-Chem

The Weather Research and Forecasting with Chemistry (WRF-Chem) model was run at 12 km × 12 km over the Continental U.S. for all days of 2019: 1 January 2019 – 31 December 2019 as described in He et al. (2024). For anthropogenic emissions, the Fuel-based Inventory of Vehicle Emissions (FIVE) was used to provide on-road and off-road mobile emissions, the Fuel-based Oil and Gas (FOG) inventory was used for emissions associated with oil and natural gas production, power plant emissions were provided by Continuous Emissions Monitoring Systems (CEMS), and all other anthropogenic emissions were obtained from the 2014 or 2017 National Emissions Inventory (NEI). Biogenic emissions were estimated using Biogenic Emissions Inventory System (BEIS) version 3.13. Gas-phase chemistry was from the RACM_ESRL_VCP scheme. Boundary conditions were provided from the Realtime Air Quality Modeling System (RAQMS, http://raqms-ops.ssec.wisc.edu/) developed by the University of Wisconsin-Madison. The cloud fractions used in this project are from the total cloud fraction "CLDFRA" variable.

https://doi.org/10.5194/egusphere-2025-1350
Preprint. Discussion started: 15 April 2025

3 Results

3.1 CONUS Cloud Patterns

We first conduct an analysis of cloud patterns across the contiguous United States, and inter-compare clear-sky days estimated by TROPOMI, the ERA5 re-analysis, and the WRF-Chem model (Figure 1). For TROPOMI, we define clear skies as the percentage of days with qa_value > 0.75, which almost exclusively filters based on cloud fractions <0.5; cloud-free snow-covered scenes typically have a qa_value > 0.75 (Eskes et al., 2022). For ERA5 and WRF-Chem, we define clear skies as the percentage of days with the total cloud fractions <0.5. ERA5 and WRF-Chem have similar clear-sky spatial patterns as TROPOMI but show systematically lower amounts of clear-skies by 8%. The small systematic difference between TROPOMI and ERA5 when filtering for cloud fractions at 13:30 is likely driven by how optically thin cirrus-like clouds are handled; for TROPOMI these are being observed based on optical properties and therefore optically thin clouds are not assumed to be a cloud, whereas in weather models (ERA5 and WRF-Chem) these are being computed as vertical layers in the atmosphere with condensed water vapor. Overall, there is very strong agreement between the three datasets in the estimation of clouds giving us confidence that TROPOMI, ERA5, and WRF-Chem are all good estimators of daily clear-sky amounts.

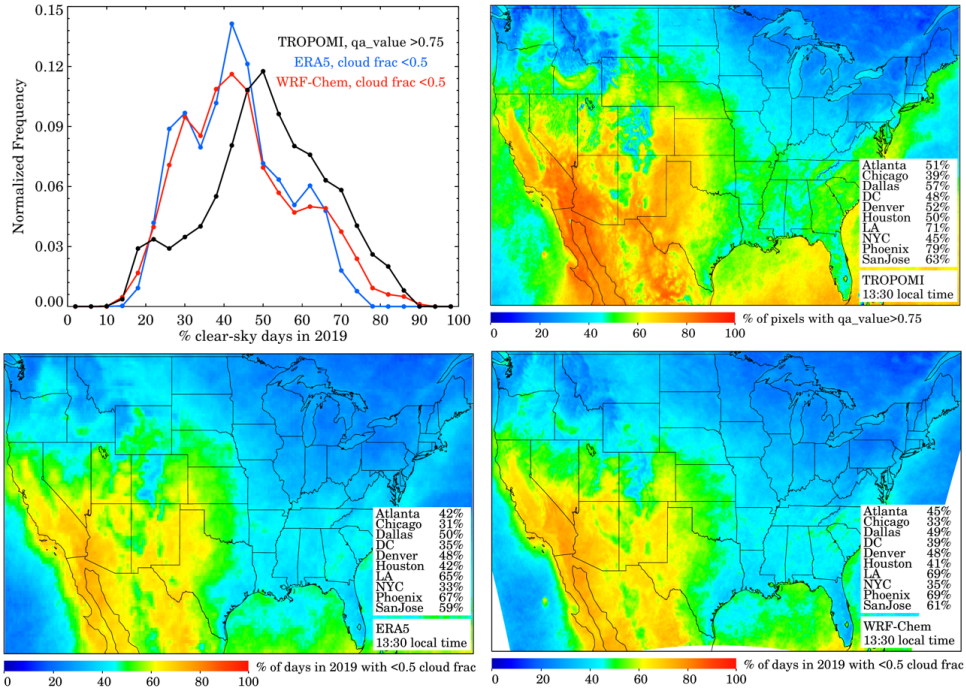

Figure 1. Percentage of clear-sky days over the contiguous U.S. during 2019 from the TROPOMI NO_2 v2.4 product, ERA5 re-analysis, and WRF-Chem. (Top left) Normalized frequency diagram of the binned percentage of clear sky days for the three products. (Top right) Percentage of days in which the qa_value of the TROPOMI NO_2 v2.4 measurement was greater than 0.75. (Bottom left) Percentage of days in which the total cloud cover (tcc) from the ERA5 was less than 0.5. (Bottom right) Percentage of days in each grid cell in which the total cloud fraction from the WRF-Chem was less than 0.5

https://doi.org/10.5194/egusphere-2025-1350
Preprint. Discussion started: 15 April 2025

For the remainder of this project, we define "clear sky" based on the TROPOMI NO_2 retrieval and use days with observations exceeding a qa_value of 0.75. According to TROPOMI – which is the only true observational dataset – the Southwest U.S. has the most amount of clear-sky days per year (~80% of days at 13:30 local time), while the interior Northeast U.S. and coastal Northwest has the fewest (~30% of days at 13:30 local time). The major U.S. city with the most clear-sky days is Phoenix (79% of days), while the major U.S. city with the least clear-sky days is Seattle (29% of days).

Annualized spatial cloud patterns are similar throughout the daylight hours with marginally more clear skies in the morning hours especially in the eastern U.S (Figure S1). Despite this, clouds are often transient, and there are opportunities to observe a clear sky measurement at a different hour of the day if the 13:30 observation is obstructed by clouds. In Figure 2, we demonstrate that between 68% – 93% of days have a clear sky measurement during any hour of the daytime as compared to the 33 – 69% range at 13:30.

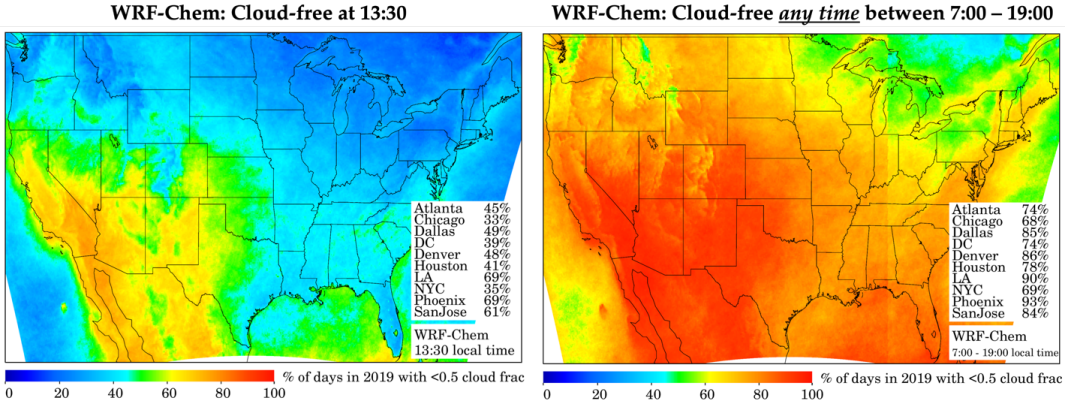

Figure 2. Percentage of days over the contiguous U.S. during 2019 with cloud fractions less than 0.5 as simulated by WRF-Chem at various local times: (Left) 13:30, (Right) any time between 7:00 – 19:00.

3.2 Surface NO_2: Clouds vs. No Clouds

We then link whether TROPOMI is observing a clear sky or not (i.e., qa_value > 0.75) to the daily *in situ* ground-level NO_2 observations to determine how clouds are affecting surface NO_2 concentrations (hereafter referred to as surface NO_2). In Figure 3, we show that surface NO_2 at 13:30 local time is +12.9% larger (NMC = normalized mean change) [–3.8% (10^{th} percentile), +32.1% (90^{th} percentile)] on days with clouds at 13:30 compared to the annualized 13:30 average when all days of data are included. We also note the very strong correlation between the NO_2 on cloudy days and all days, which suggests that the presence of clouds drives a systematic change from the mean rather than a random change. We next show that the NO_2 during the average of all days is +17.2% larger [–1.8%, +38.7%] than on days with only clear skies. The +17.2% value is our estimate of the difference of annualized surface-based NO_2 at 13:30 on all days as compared to only clear sky days. We further show that surface NO_2 at 13:30 is +36.0% larger [–6.1%, +72.9%] on days with clouds compared to days with clear skies.

https://doi.org/10.5194/egusphere-2025-1350
Preprint. Discussion started: 15 April 2025

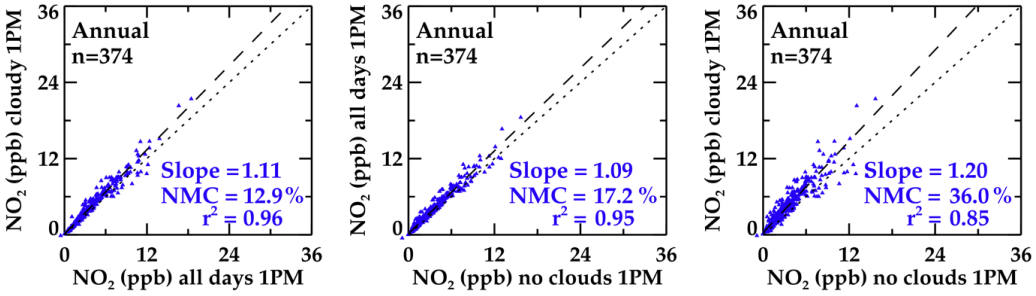

Figure 3. Scatterplots intercomparing annualized surface NO_2 from the EPA AQS at 13:30 local time during all days, cloudy days, and no cloud days. (Left) Annualized surface NO_2 during cloudy days compared to annualized surface NO_2 during all days. (Center) Annualized surface NO_2 during all days compared to annualized surface NO_2 during no cloud days. (Right) Annualized surface NO_2 during cloudy days compared to annualized surface NO_2 during no cloud. A "cloudy" vs "no cloud" day is determined via the qa_value of 0.75 from the TROPOMI NO_2 v2.4 product.

The difference in surface NO_2 between cloudy and clear sky days can vary dramatically based on geographic region and proximity to a major roadway (Table 1). For the purposes of the sensitivity study, we focus on the cloudy versus no cloud days, while the directional changes of "cloudy versus all days" and "all days versus no clouds" values are similar (Tables S1 & S2).

Table 1. Slope, r^2, Normalized Mean Change (NMC), and number of sites of the "cloudy vs. no clouds" bias by further filtering out AQS data using various additional sensitivity analyses. Tables S1 & S2 show the sensitivity analyses for the "cloudy vs. all days" bias, and "all days vs. no clouds" bias respectively.

	Slope	r^2	Normalized Mean Change (%)	# sites of monitoring sites used
Baseline (V2.4)	1.20	0.85	+36.0%	374
V2.3.1	1.18	0.86	+40.4%	374
V2.4 higher cloud filter	1.25	0.83	+80.8%	373
V2.4 all sites	1.05	0.90	+32.7%	449
V2.4 near road only	0.89	0.84	+15.9%	76
V2.4 no chemiluminescence	1.20	0.87	+53.1%	26
V2.4 Summer only	1.17	0.86	+23.8%	366
V2.4 Winter only	1.14	0.82	+27.8%	373
V2.4 Spring only	1.28	0.88	+31.9%	364
V2.4 Fall only	1.07	0.77	+30.9%	359
V2.4 North only	1.31	0.89	+41.5%	217
V2.4 South only	0.98	0.82	+28.5%	157
V2.4 NorthEast only	1.36	0.93	+61.7%	106
V2.4 SouthEast only	1.27	0.94	+33.8%	73
V2.4 NorthWest only	1.12	0.88	+22.2%	111
V2.4 SouthWest only	0.91	0.79	+23.9%	84
V2.4 lowPopDensity only	1.34	0.86	+36.3%	216
V2.4 highPopDensity only	1.13	0.76	+37.5%	167
V2.4 lowRoadDensity only	1.19	0.82	+33.6%	216
V2.4 highRoadDensity only	1.18	0.80	+40.8%	165

https://doi.org/10.5194/egusphere-2025-1350
Preprint. Discussion started: 15 April 2025

First, we find that NO_2 during cloudy days is larger in the northern U.S. (+41.5%) than the southern U.S. (+28.5%) and largest in the Northeast U.S (+61.7%) (Figure 4); for this analysis, 37°N is the dividing latitude between North and South, 100°W is the dividing longitude between East and West. Although the calculated cloudy versus no cloud change is independent of the number of days of clear-skies, areas of perpetually cloudy skies also have cooler temperatures and shallower boundary layers which could cause much larger NO_2 on cloudy days. Interestingly, the Phoenix and Salt Lake City areas – two areas with large number of days with clear skies – also have a relatively large difference between cloudy and clear sky days demonstrating that the bias in independent of the number of days with clear skies. However, the *annualized* difference between cloudy and clear sky days in the Southwest U.S. is modest (+4.8%) (Table S1) because there are fewer individual days affected by clouds. Approximately 13% of monitoring sites, mostly concentrated in the Los Angeles and San Diego areas, have lower NO_2 on cloudy days, and this may be driven by enhanced westerly winds on cloudy days bringing in cleaner marine air more than offsetting the photochemically driven larger NO_2 on cloudy days. Overall, while there are a few locations with lower NO_2 on cloudy days, 87% of locations exhibit larger NO_2 on cloudy days and this is driven by the slower photochemistry on these days.

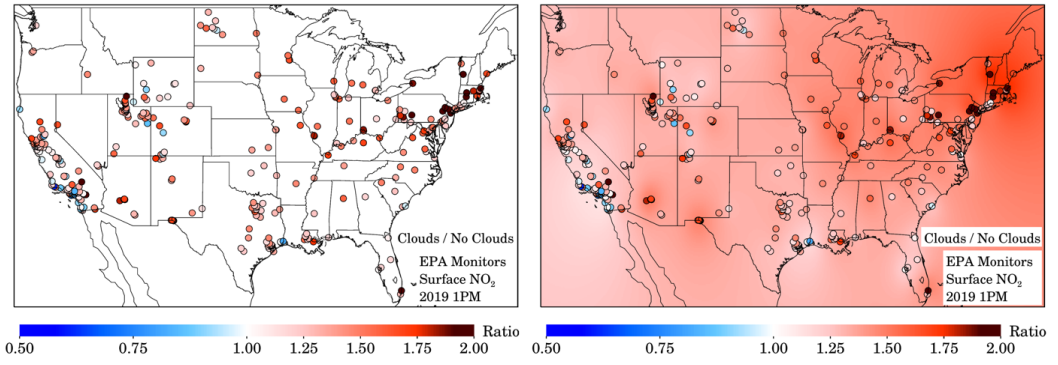

Figure 4. (Left) Ratio of the annualized surface NO_2 during cloudy and no cloud days at the EPA AQS sites not classified as "near-road". (Right) Same image but with an inverse distance weighting underlaid to infer geographic distribution of the ratio.

Proximity to roadways and large sources of NOx is another driver of whether a location will experience a small (but larger) difference in NO_2 on cloudy and clear sky days. For areas in close proximity to roadways (i.e., the near-road sites) (n=76), the difference in NO_2 between cloudy and clear sky days is weaker: a smaller positive change (+15.9%) and only 77% of sites displaying a positive mean change, which is less than the difference at all other NO_2 monitoring locations (+36.0%).

We find that seasonal effects on the differences in NO_2 between cloudy and clear days are modest. The NO_2 on cloudy days in the Spring is largest and marginally smaller in other seasons. Other factors that were not associated with strong changes to the differences in NO_2 between cloudy and clear days bias are: the version of the TROPOMI NO_2 algorithm,

https://doi.org/10.5194/egusphere-2025-1350
Preprint. Discussion started: 15 April 2025

whether the site was using a chemiluminescence or Cavity Attenuated Phase Shift measurement technique, and population / roadway density within a 0.5° radius.

3.3 TROPOMI NO_2: Clouds versus No Clouds

We then compare TROPOMI NO_2 measurements under varying sky conditions. For this exercise, we filter the TROPOMI NO_2 data strictly based on cloud radiative fraction (crf). Although it is recommended for most applications to use data when the crf <0.5, sometimes measurements are usable in the presence of optically thick clouds (i.e., crf >0.5). In Figure 5, we average TROPOMI NO_2 measurements below and above a crf = 0.5 threshold to gain an understanding of how TROPOMI column NO_2 measurements intercompare in the presence and lack of optically thick clouds. In the figure we show the tropospheric vertical columns on the top row, and tropospheric slant columns in the middle row, which have been interconverted using the tropospheric air mass factor shown on the bottom row. As discussed in Section 2.2.1, the tropospheric air mass factor can be a large source of uncertainty when calculating tropospheric vertical columns from slant columns (Glissenaar et al., 2025; S. Liu et al., 2021; Rijsdijk et al., 2025).

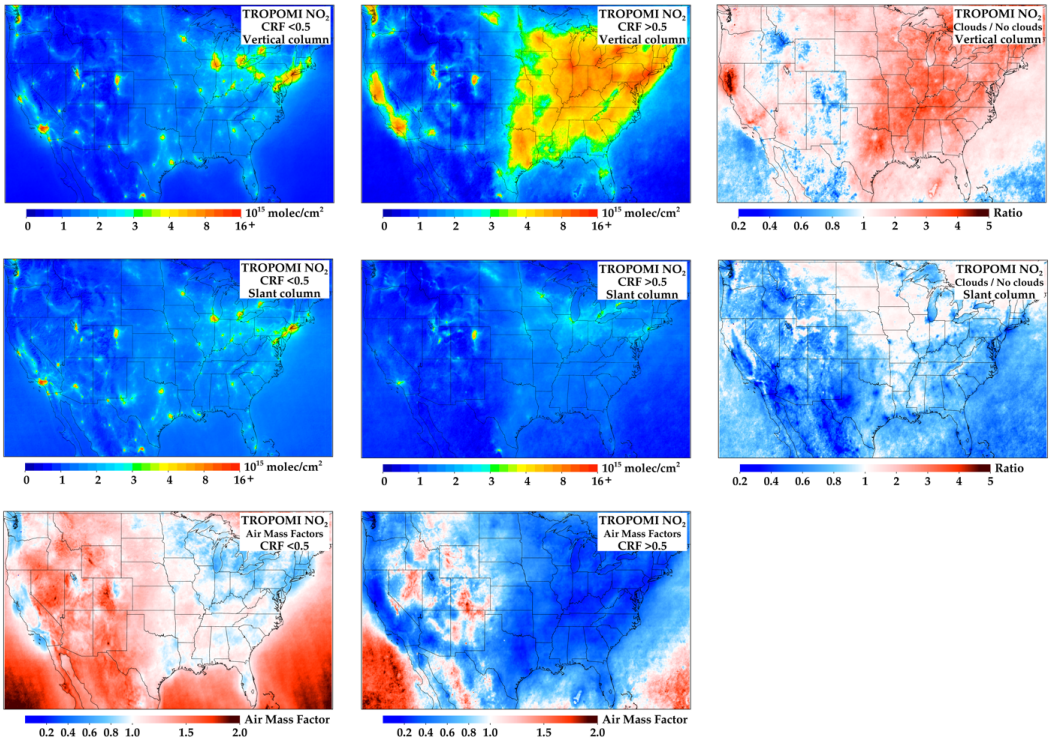

Figure 5. (Left column) Annual 2019 TROPOMI NO_2 filtered using only a cloud radiative fraction (crf) filter less than 0.5. (Center column) Annual 2019 TROPOMI NO_2 filtered using only a crf filter greater than 0.5. (Right column) Ratio between the two annual averages. (Top row) Vertical tropospheric column NO_2 data. (Center row) Slant tropospheric column NO_2 data. (Bottom row) Tropospheric air mass factors.

https://doi.org/10.5194/egusphere-2025-1350
Preprint. Discussion started: 15 April 2025

In Figure 5, we demonstrate that the vertical column NO_2 spatial patterns in the presence of clouds are much different in magnitude than the slant column NO_2 whereas the vertical column NO_2 spatial patterns in the absence of clouds are similar to the slant column NO_2. As shown, this is primarily driven by the assumed tropospheric air mass factors. During measurements when the crf >0.5 as compared to measurements when crf <0.5, the air mass factors are smaller in magnitude. This is primarily because sensitivity to the surface concentrations is altered (lower) in the slant column measurement in the presence of clouds. Also, during measurements when the crf >0.5, the uncertainty of the TROPOMI vertical column measurements rises, and this is driven by the difficulty in calculating the air mass factor in the presence of clouds; in addition to needing to know the vertical NO_2 profile for its calculation, we also need to know the pressure level and thickness of the clouds. Such errors can generate nonlinear responses. This analysis confirms that the assumed air mass factor is the driving factor causing the differences in the tropospheric vertical column NO_2 between clear and cloudy sky days, as the slant tropospheric column NO_2 is smaller during cloudy skies due to a lack of instrument sensitivity to the surface during cloudy conditions. Therefore special care should be used when interpreting tropospheric satellite measurements in the presence of clouds.

Qualitatively, the ratio of the column NO_2 with and without clouds is spatially similar to the ratio from the AQS analysis – with the largest ratios occurring in the Northeast U.S and smallest ratios occurring in the Southwest U.S. However, quantitatively, the column ratio observed by TROPOMI is much larger in magnitude in the eastern U.S. than the surface ratio observed at the AQS surface sites. It is difficult to determine whether the quantitative magnitude is correct because there are no ground-based instruments to accurately measure column NO_2 in the presence of clouds.

3.4 WRF-Chem NO_2: Clouds vs. No Clouds

We then compare the differences in NO_2 between cloudy and clear days observed by the EPA AQS surface network to the differences in NO_2 between cloudy and clear days of surface NO_2 simulated by WRF-Chem. The 13:30 local time differences in NO_2 between cloudy and clear days of surface NO_2 in WRF-Chem (+58.7%) is substantially larger than from the AQS observations (+36.0%) during collocations. This directional change is consistent among all geographic regions suggesting that NO_2 concentrations are too responsive to sunlight in WRF-Chem.

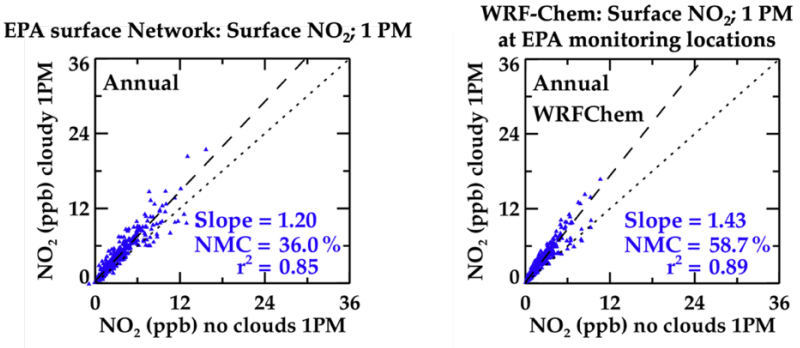

Figure 6. Scatterplots intercomparing annualized surface NO_2 at 13:30 local time during cloudy days vs. no cloud days. (Left) EPA AQS data which is a repeat of Figure 3c. (Right) WRF-Chem collocated with the AQS monitoring sites, and using the WRF-Chem cloud filter in lieu of the TROPOMI cloud filter.

https://doi.org/10.5194/egusphere-2025-1350
Preprint. Discussion started: 15 April 2025

There could be several reasons for this discrepancy. First, the NO_2 + OH reaction is often the terminal sink for NO_2 during daytime, and it is possible that OH concentrations in WRF-Chem are fluctuating too rapidly in the presence of and lack of clouds (Duncan et al., 2024). Second, there might be insufficient NO_2 recycling of organic nitrates and/or particulate nitrates in the model which could buffer photolysis-related changes; recent work has suggested that particulate nitrate can meaningfully photolyze back to NO_2 (Sarwar et al., 2024; Shah et al., 2024). Third, WRF-Chem may not simulate PBL depth properly and may have different biases during cloudy and clear sky conditions (Hegarty et al., 2018; Kuhn et al., 2024; X. Liu et al., 2023). For example if the predicted PBL is too shallow during cloudy conditions, this could be a contributing factor to the simulated surface NO_2 bias. Errors in surface jNO_2 do not appear to be a primary driver of the cloudy versus clear sky disagreements as the jNO_2 values from WRF-Chem seem reasonable as compared to UV-B measurements from the NOAA Surface Radiation Budget (SURFRAD) monitoring network (Figure S3) and is consistent with other work showing small biases in jNO_2 in WRF-Chem (Ryu et al., 2018). Follow-up work will address some of these shortcomings by adding particulate nitrate photolysis into the chemical mechanism and evaluating PBL depths during cloudy conditions using ceilometers.

We can then use WRF-Chem as a transfer standard to suggest how column NO_2 may change in relation to the surface NO_2, and we find that the relative change in column NO_2 and surface NO_2 in response to clouds are very similar (Figure 7). This makes intuitive sense because most NO_2 over the contiguous U.S. is located within the boundary layer, and typically clouds (if they exist) are located at the top of the boundary layer. So any sunlight obstructed by clouds will also obstruct the NO_2 both at the surface and in the full boundary layer.

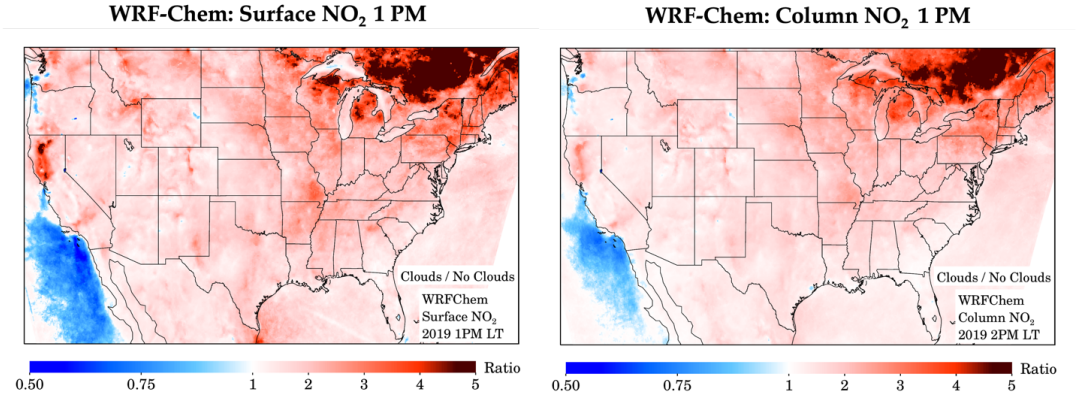

Figure 7. Ratio of the annualized surface NO_2 at 13:30 local time from WRF-Chem during cloudy and no cloud days. (Left) Surface NO_2 (Right) Tropospheric column NO_2.

https://doi.org/10.5194/egusphere-2025-1350
Preprint. Discussion started: 15 April 2025

3.5 Impacts of clouds on geostationary observations

Finally, we use provisional TEMPO NO_2 data and AQS NO_2 data from 2 August 2023 through 31 August 2024 to understand how the changes of NO_2 during clear and cloudy conditions may be altered at different hours of the day. Any hour in which there was high quality TEMPO NO_2 data was assumed to be "clear sky", while all other days are assumed to be cloudy. The threshold between high quality and lower quality data is a cloud radiative fraction =0.15, which is more stringent than the TROPOMI recommendation. Hours with low solar zenith angles (before 8:00 and after 16:00) have been excluded from this analysis. We find that the difference in surface NO_2 between clear and cloudy days is negligible in the early morning hours and increases throughout the day (Figure 8).

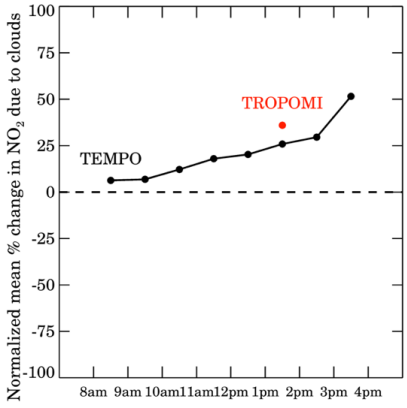

Figure 8. Normalized mean percentage change in the surface NO_2 during days with cloudy skies as opposed to days with clear skies. Red dot shows the mean percentage change using TROPOMI clouds as shown in Figure 2c. Black line uses the same procedure for Aug 2023 – July 2024 data and TEMPO cloud data.

Surface AQS NO_2 at 8:30 local time is +6.3% larger on cloudy days than clear sky days, while at 15:30 it is +51.6% larger. The calculated 13:30 difference in surface NO_2 between cloudy and clear sky days using TEMPO (+25.9%) is similar to the analogous value from TROPOMI (+36.0%). Differences between TEMPO and TROPOMI are expected because the timeframes for the analyses are different (2019 for TROPOMI and 2023-2024 for TEMPO), and because the cloud algorithms and cloud screening recommendations between the two instruments are different. The recommended TEMPO cloud fraction threshold for high quality data is more stringent (crf=0.15) and therefore some days with mostly clear skies are assumed to be "cloudy" in the TEMPO analysis. Therefore it is expected that the normalized mean percentage change of the AQS NO_2 using TEMPO clouds is lower than the analogous value using TROPOMI clouds since the theoretical difference between "clear" and "cloudy" days is less stark.

4 Discussion

In this project we quantify how NO_2 satellite data could be biased in estimating annualized surface NO_2 concentrations due to having high quality measurements only in the absence of clouds. We find that surface *in situ* NO_2 measurements are on average +17% on all days compared to restricting to clear sky days and +36% larger during cloudy days vs. clear sky days, with a wide distribution based on geographic region and proximity to

https://doi.org/10.5194/egusphere-2025-1350
Preprint. Discussion started: 15 April 2025

roadway. Using the United States as a case study, we find the clear-sky bias to be largest in the Northeast U.S.; conversely, the clear-sky bias is smallest in the Southwest U.S. and near major roadways. In some areas of the urban Western U.S., Los Angeles and San Diego, we find that NO_2 is lower on cloudy days, but these instances are rare (13% of monitoring sites) and are driven by unique transport patterns on cloudy days. Transport patterns are a significant driver of the regional clear vs. cloudy sky differences of surface NO_2 concentrations. Although the analysis was computed for both TROPOMI and TEMPO data, it should be re-emphasized that the cloud algorithms used by both instruments are different. However, the qualitative finding that surface NO_2 differences between cloudy and clear conditions tend to be larger in the afternoon than morning is consistent with a hypothesis that active photochemistry during periods of stronger afternoon sunlight would cause this change.

This work also highlights how NO_2 concentrations are different on days when satellite instruments are not acquiring a valid measurement. Our initial hypothesis of NO_2 being consistently larger on cloudy days was only partially proven true. In many cases, surface NO_2 concentrations and column NO_2 are larger, but this is not always the case. This project demonstrates the balancing act of the reduced NO_2 + OH sink and local climatological patterns (wind speed/direction, PBL depth, etc.) driving surface NO_2 during cloudy conditions. Although one of the original goals of this study was to better gap-fill satellite tropospheric vertical column NO_2 measurements in the presence of clouds, ultimately, we were not comfortable doing this yet. Reliance on a model as a transfer standard to convert surface concentrations into column concentrations exhibited too many biases under cloudy conditions. WRF-Chem model simulations of surface NO_2 suggest that the clear-sky bias in WRF-Chem is on average much larger than the observed clear-sky bias: +59% on cloudy days vs. clear days for the model, and +36% for the AQS data. We hypothesized that errors in OH chemistry, NO_2 recycling speeds, and PBL mixing depths could all be contributing to this high bias. Future work should target these three research topics. Future work could also use a machine-learning approach to account for some of these model biases.

Another consideration with the interpretation of satellite measurements is the impact of lightning NOx, wildfire NOx, and aircraft NOx emissions, mostly staying aloft, which could be misinterpreted as surface NO_2 enhancements. While lightning NOx and wildfire NOx emissions are often screened out when applying a cloud filter because they occur in optically thick clouds/smoke, it is possible for the NO_2 to remain aloft for several days after the initial thunderstorm/fire and be observed during clear skies. An algorithm to detect and screen out downwind NO_2 attributed to upwind lightning NOx and wildfire NOx emissions could be especially helpful for subtropical and tropical areas. At minimum, care should be taken during timeframes and regions where there are large pulses of these types of emissions, such as our findings during summer.

These results have repercussions for many applied studies that use satellite data to estimate surface NO_2 concentrations or NOx emissions. First, for studies that estimate surface concentrations, it is important to ingest surface NO_2 measurements during cloudy (and nighttime) conditions in some capacity in order to appropriately estimate 24-hour concentrations; most studies already do this. If one were to use the clear-sky satellite data coupled with only a chemical transport model as a transfer standard to convert the column measurement into a pseudo-

https://doi.org/10.5194/egusphere-2025-1350
Preprint. Discussion started: 15 April 2025

surface "measurement", this would underestimate annualized NO_2 concentration in most places. Unfortunately, there are many global regions with few or no surface measurements, so this is an important consideration when estimating surface NO_2 in these regions. But even if one were to ingest surface NO_2 during cloudy conditions, the spatial patterns of surface NO_2 during cloudy conditions may be slightly different than implied by the clear-sky satellite data. For example, we find that NO_2 surface concentrations under cloudy conditions are much larger in the Northeast U.S. than the Southwest U.S., and a cloud-free satellite map does not capture this.

Second, for nitrogen oxide emissions estimates it is often assumed that anthropogenic emission rates are similar under cloudy and clear-sky conditions, but this is likely not the case in reality. Although we show that surface NO_2 concentrations are typically smaller under clear-skies, it is likely that anthropogenic NOx emissions are actually larger under regionwide clear-skies during summer and winter due to the moderating impact of clouds on surface temperature and subsequent impacts on heating-ventilation-air conditioning (HVAC) usage/emissions (Abel et al., 2017). If we were able to better independently estimate tropospheric vertical column NO_2 during cloudy conditions, perhaps this could be investigated in the future.

Lastly, as satellite-derived NO_2 applications increase over the coming years, it is important to document its successes and shortcomings. We see this project as a first-step towards better accounting for the clear-sky bias of satellite NO_2 data. While future NO_2 applications may use geostationary data, such as TEMPO, which may suffer from a similar bias depending on the hour of the day, an advantage of geostationary satellite data is the ability to use multiple measurements per day before and just after the clouds. It might be possible to isolate a two-hour window (one with a cloud and one without) to get a better handle on the instantaneous versus long-term role of clouds affecting NO_2 concentrations.

This work also highlights the critical role that chemical transport models can play in satellite NO_2 applications. Errors in the model assumptions can hamstring many NO_2 applications. For example, using a model to infer NO_2 during cloudy conditions in the lack of clear-sky satellite data would yield significant errors. Therefore, future work should concurrently focus on acquiring and using sub-orbital measurements to diagnose errors related in simulating NO_2 in chemical transport models, so that they can be used as more robust transfer standards.

https://doi.org/10.5194/egusphere-2025-1350
Preprint. Discussion started: 15 April 2025

Data availability. TROPOMI NO_2 version 2.4 data (http://doi.org/10.5270/S5P-9bnp8q8) processed to 0.01° × 0.01° resolution (http://doi.org/10.5067/MKJG22GUOD34) and TEMPO NO_2 version 3 data (http://doi.org/10.5067/IS-40e/TEMPO/NO2_L3.003) can be freely downloaded from NASA Earthdata. EPA AQS surface NO_2 data can be downloaded from pre-generated files: https://aqs.epa.gov/aqsweb/airdata/download_files.html. ERA5 re-analysis hourly data on single levels (http://doi.org/10.24381/cds.adbb2d47) can be downloaded from Copernicus Climate Data Store (https://cds.climate.copernicus.eu/#!/home). NOAA SURFAD data can be downloaded from: https://gml.noaa.gov/grad/surfrad/sitepage.html . Output from the WRF-Chem simulation is available upon request. IDL code to process the data is available upon request.

Author contribution. D.G., A.C., S.K., and S.A. developed the project design. J.H. and C.L. set-up and conducted the WRF-Chem simulations. D.G downloaded and processed the TROPOMI NO_2, TEMPO NO_2, ERA5, and SURFRAD data and re-gridded all data to a standardized grid. M.O.N. helped to process the surface NO_2 data. D.G. developed all figures for the manuscript and wrote the paper. All authors edited the manuscript.

Competing interests. The contact author has declared that none of the authors have any competing interests.

Acknowledgments. Preparation of this manuscript was funded by grants from the NOAA GeoXO program (1305M323PNRMA0668) and the NASA Health and Air Quality Applied Sciences Team (HAQAST) (80NSSC21K0511). NOAA Cooperative Agreement (NA17OAR4320101 and NA22OAR4320151) funded C. Lyu and J. He. The WRF-Chem simulation was supported by NOAA's High Performance Computing Program. The authors would also like to thank Brian McDonald and Laura Judd for very helpful feedback during preparation of this manuscript.

Supporting Information. The supporting information includes: 1) a spatial plot of the annual average of days with total cloud fraction less 0.5 as simulated by WRF-Chem during 8 AM, 1 PM, and 5 PM local time, 2) scatterplots of various 2019 annual averages of surface NO_2 and TROPOMI NO_2 measurements, 3) jNO_2 from WRF-Chem and an intercomparison with the NOAA SURFRAD network, 4) Tables of "cloudy vs. all days" and "all days vs. no clouds" analogous to Table 1 which shows "cloudy vs. no clouds".

https://doi.org/10.5194/egusphere-2025-1350
Preprint. Discussion started: 15 April 2025

References

Abel, D. W., Holloway, T., Kladar, R. M., Meier, P., Ahl, D., Harkey, M., & Patz, J. (2017). Response of Power Plant Emissions to Ambient Temperature in the Eastern United States. *Environmental Science and Technology*, *51*(10), 5838–5846. https://doi.org/10.1021/acs.est.6b06201

Acker, S. J., Holloway, T., & Harkey, M. K. (2025, February 13). Satellite Detection of NO2 Distributions and Comparison with Ground-Based Concentrations. *EGUsphere*. https://doi.org/10.5194/egusphere-2025-226

Anenberg, S. C., Mohegh, A., Goldberg, D. L., Kerr, G. H., Brauer, M., Burkart, K., et al. (2022). Long-term trends in urban NO2 concentrations and associated paediatric asthma incidence: estimates from global datasets. *The Lancet Planetary Health*, *6*(1), e49–e58. https://doi.org/10.1016/S2542-5196(21)00255-2

Bechle, M. J., Millet, D. B., & Marshall, J. D. (2015). National Spatiotemporal Exposure Surface for NO2: Monthly Scaling of a Satellite-Derived Land-Use Regression, 2000-2010. *Environmental Science and Technology*, *49*(20), 12297–12305. https://doi.org/10.1021/acs.est.5b02882

Boersma, K. F., Eskes, H. J., Dirksen, R. J., Van Der A, R. J., Veefkind, J. P., Stammes, P., et al. (2011). An improved tropospheric NO2 column retrieval algorithm for the Ozone Monitoring Instrument. *Atmospheric Measurement Techniques*, *4*(9), 1905–1928. https://doi.org/10.5194/amt-4-1905-2011

Burnett, R. T., Stieb, D., Brook, J. R., Cakmak, S., Dales, R., Raizenne, M., et al. (2004). Associations between short-term changes in nitrogen dioxide and mortality in Canadian cities. *Archives of Environmental Health*, *59*(5), 228–236. https://doi.org/10.3200/AEOH.59.5.228-236

Busca, G., Lietti, L., Ramis, G., & Berti, F. (1998). Chemical and mechanistic aspects of the selective catalytic reduction of NO(x) by ammonia over oxide catalysts: A review. *Applied Catalysis B: Environmental*, *18*(1–2), 1–36. https://doi.org/10.1016/S0926-3373(98)00040-X

Crippa, M., Guizzardi, D., Pisoni, E., Solazzo, E., Guion, A., Muntean, M., et al. (2021). Global anthropogenic emissions in urban areas: patterns, trends, and challenges. *Environmental Research Letters*, *16*(7), 074033. https://doi.org/10.1088/1748-9326/AC00E2

Demetillo, M. A. G., Navarro, A., Knowles, K. K., Fields, K. P., Geddes, J. A., Nowlan, C. R., et al. (2020). Observing Nitrogen Dioxide Air Pollution Inequality Using High-Spatial-Resolution Remote Sensing Measurements in Houston, Texas. *Environmental Science & Technology*, *54*(16), 9882–9895. https://doi.org/10.1021/acs.est.0c01864

Dickerson, R. R., Anderson, D. C., & Ren, X. (2019). On the use of data from commercial NOx analyzers for air pollution studies. *Atmospheric Environment*, *214*, 116873. https://doi.org/10.1016/j.atmosenv.2019.116873

Dressel, I. M., Demetillo, M. A. G., Judd, L. M., Janz, S. J., Fields, K. P., Sun, K., et al. (2022). Daily Satellite Observations of Nitrogen Dioxide Air Pollution Inequality in New York City, New York and Newark, New Jersey: Evaluation and Application. *Environmental Science and Technology*, *2022*. https://doi.org/10.1021/ACS.EST.2C02828/ASSET/IMAGES/LARGE/ES2C02828_0006.JPEG

Duncan, B. N., Anderson, D. C., Fiore, A. M., Joiner, J., Krotkov, N. A., Li, C., et al. (2024). Opinion: Beyond global means – novel space-based approaches to indirectly constrain the concentrations of and trends and variations in the tropospheric hydroxyl radical (OH). *Atmospheric Chemistry and Physics*, *24*(22), 13001–13023. https://doi.org/10.5194/acp-24-13001-2024

https://doi.org/10.5194/egusphere-2025-1350
Preprint. Discussion started: 15 April 2025

513 Eskes, H., van Geffen, J., Boersma, F., Eichman, K., Apituley, A., Pedergnana, M., et al. (2022). *Sentinel-5*
514 *precursor/TROPOMI Level 2 Product User Manual Nitrogendioxide*.

515 de Foy, B., Krotkov, N. A., Bei, N., Herndon, S. C., Huey, L. G., Martínez, A.-P., et al. (2009). Hit from both sides:
516 tracking industrial and volcanic plumes in Mexico City with surface measurements and OMI SO2 retrievals
517 during the MILAGRO field campaign. *Atmospheric Chemistry and Physics*, *9*(24), 9599–9617.
518 https://doi.org/10.5194/acp-9-9599-2009

519 Geddes, J. A., Murphy, J. G., O'Brien, J. M., & Celarier, E. A. (2012). Biases in long-term NO2 averages inferred
520 from satellite observations due to cloud selection criteria. *Remote Sensing of Environment*, *124*(2), 210–216.
521 https://doi.org/10.1016/j.rse.2012.05.008

522 van Geffen, J. (2016). TROPOMI ATBD of the total and tropospheric NO2 data products, (2). Retrieved from
523 https://sentinel.esa.int/documents/247904/2476257/Sentinel-5P-TROPOMI-ATBD-NO2-data-products

524 van Geffen, J., Boersma, K. F., Eskes, H. J., Sneep, M., ter Linden, M., Zara, M., & Veefkind, J. P. (2020). S5P
525 TROPOMI NO2 slant column retrieval: method, stability, uncertainties and comparisons with OMI.
526 *Atmospheric Measurement Techniques*, *13*(3), 1315–1335. https://doi.org/10.5194/amt-13-1315-2020

527 van Geffen, J., Eskes, H. J., Compernolle, S., Pinardi, G., Verhoelst, T., Lambert, J.-C., et al. (2021). Sentinel-5P
528 TROPOMI NO2 retrieval: impact of version v2.2 improvements and comparisons with OMI and ground-based
529 data. *Atmospheric Measurement Techniques*, *15*(7), 2037–2060. https://doi.org/10.5194/AMT-15-2037-2022

530 Glissenaar, I., Folkert Boersma, K., Anglou, I., Rijsdijk, P., Verhoelst, T., Compernolle, S., et al. (2025). TROPOMI
531 Level 3 tropospheric NO2 Dataset with Advanced Uncertainty Analysis from the ESA CCI+ ECV Precursor
532 Project. *EGUsphere*. https://doi.org/10.21944/CCI-NO2-TROPOMI-L3

533 Goldberg, D. L., Anenberg, S. C., Kerr, G. H., Mohegh, A., Lu, Z., & Streets, D. G. (2021). TROPOMI NO2 in the
534 United States: A Detailed Look at the Annual Averages, Weekly Cycles, Effects of Temperature, and
535 Correlation With Surface NO 2 Concentrations. *Earth's Future*, *9*(4), e2020EF001665.
536 https://doi.org/10.1029/2020EF001665

537 Goldberg, D. L., Harkey, M., de Foy, B., Judd, L., Johnson, J., Yarwood, G., & Holloway, T. (2022). Evaluating
538 NOx emissions and their effect on O3 production in Texas using TROPOMI NO2 and HCHO. *Atmospheric*
539 *Chemistry and Physics*, *22*(16), 10875–10900. https://doi.org/10.5194/acp-22-10875-2022

540 Goldberg, D. L., Tao, M., Kerr, G. H., Ma, S., Tong, D. Q., Fiore, A. M., et al. (2024). Evaluating the spatial
541 patterns of U.S. urban NOx emissions using TROPOMI NO2. *Remote Sensing of Environment*, *300*, 113917.
542 https://doi.org/10.1016/j.rse.2023.113917

543 Harkey, M., & Holloway, T. (2024). Simulated Surface-Column NO2 Connections for Satellite Applications.
544 *Journal of Geophysical Research: Atmospheres*, *129*(21). https://doi.org/10.1029/2024JD041912

545 He, J., Harkins, C., O'Dell, K., Li, M., Francoeur, C., Aikin, K. C., et al. (2024). COVID-19 perturbation on US air
546 quality and human health impact assessment. *PNAS Nexus*, *3*(1). https://doi.org/10.1093/pnasnexus/pgad483

547 He, M. Z., Kinney, P. L., Li, T., Chen, C., Sun, Q., Ban, J., et al. (2020). Short- and intermediate-term exposure to
548 NO2 and mortality: A multi-county analysis in China. *Environmental Pollution*, *261*, 114165.
549 https://doi.org/10.1016/j.envpol.2020.114165

https://doi.org/10.5194/egusphere-2025-1350
Preprint. Discussion started: 15 April 2025

Health Effects Institute. (2022). *Systematic Review and Meta-analysis of Selected Health Effects of Long-Term Exposure to Traffic-Related Air Poll*. Retrieved from https://www.healtheffects.org/system/files/hei-special-report-23-executive-summary_0.pdf

Hegarty, J. D., Lewis, J., McGrath-Spangler, E. L., Henderson, J., Scarino, A. J., DeCola, P., et al. (2018). Analysis of the Planetary Boundary Layer Height during DISCOVER-AQ Baltimore–Washington, D.C., with Lidar and High-Resolution WRF Modeling. *Journal of Applied Meteorology and Climatology*, *57*(11), 2679–2696. https://doi.org/10.1175/JAMC-D-18-0014.1

Hersbach, H., Bell, B., Berrisford, P., Hirahara, S., Horányi, A., Muñoz-Sabater, J., et al. (2020). The ERA5 global reanalysis. *Quarterly Journal of the Royal Meteorological Society*, *146*(730), 1999–2049. https://doi.org/10.1002/qj.3803

Jin, X., Zhu, Q., & Cohen, R. C. (2021). Direct estimates of biomass burning NOx emissions and lifetimes using daily observations from TROPOMI. *Atmospheric Chemistry and Physics*, *21*(20), 15569–15587. https://doi.org/10.5194/acp-21-15569-2021

Kebabian, P. L., Wood, E. C., Herndon, S. C., & Freedman, A. (2008). A practical alternative to chemiluminescence-based detection of nitrogen dioxide: Cavity attenuated phase shift spectroscopy. *Environmental Science and Technology*, *42*(16), 6040–6045. https://doi.org/10.1021/es703204j

Kelly, K. E., Whitaker, J., Petty, A., Widmer, C., Dybwad, A., Sleeth, D., et al. (2017). Ambient and laboratory evaluation of a low-cost particulate matter sensor. *Environmental Pollution*, *221*, 491–500. https://doi.org/10.1016/j.envpol.2016.12.039

Kenagy, H. S., Sparks, T. L., Ebben, C. J., Wooldrige, P. J., Lopez-Hilfiker, F. D., Lee, B. H., et al. (2018). NOx Lifetime and NOy Partitioning During WINTER. *Journal of Geophysical Research: Atmospheres*, *123*(17), 9813–9827. https://doi.org/10.1029/2018JD028736

Kerr, G. H., Goldberg, D. L., Harris, M. H., Henderson, B. H., Hystad, P., Roy, A., & Anenberg, S. C. (2023). Ethnoracial Disparities in Nitrogen Dioxide Pollution in the United States: Comparing Data Sets from Satellites, Models, and Monitors. *Environmental Science & Technology*. https://doi.org/10.1021/acs.est.3c03999

Khreis, H., Kelly, C., Tate, J., Parslow, R., Lucas, K., & Nieuwenhuijsen, M. (2017). Exposure to traffic-related air pollution and risk of development of childhood asthma: A systematic review and meta-analysis. *Environment International*, *100*, 1–31. https://doi.org/10.1016/j.envint.2016.11.012

Kim, E. J., Holloway, T., Kokandakar, A., Harkey, M., Elkins, S., Goldberg, D. L., & Heck, C. (2024). A Comparison of Regression Methods for Inferring Near-Surface NO_2 With Satellite Data. *Journal of Geophysical Research: Atmospheres*, *129*(16). https://doi.org/10.1029/2024JD040906

Koltsakis, G., & Stamatelos, A. (1997). Catalytic automotive exhaust aftertreatment. *Progress in Energy and Combustion Science*, *23*(1), 1–39. https://doi.org/10.1016/s0360-1285(97)00003-8

Kuhn, L., Beirle, S., Kumar, V., Osipov, S., Pozzer, A., Bösch, T., et al. (2024). On the influence of vertical mixing, boundary layer schemes, and temporal emission profiles on tropospheric NO2 in WRF-Chem – comparisons to in situ, satellite, and MAX-DOAS observations. *Atmospheric Chemistry and Physics*, *24*(1), 185–217. https://doi.org/10.5194/acp-24-185-2024

Lambert, J.-C., Claas, J., Stein-Zweers, D., Ludewig, A., Loyola, D., Sneep, M., & Dehn, A. (2023). *Quarterly Validation Report of the Copernicus Sentinel-5 Precursor Operational Data Products #19*.

https://doi.org/10.5194/egusphere-2025-1350
Preprint. Discussion started: 15 April 2025

590 Larkin, A., Anenberg, S., Goldberg, D. L., Mohegh, A., Brauer, M., & Hystad, P. (2023). A global spatial-temporal
591 land use regression model for nitrogen dioxide air pollution. *Frontiers in Environmental Science*, *11*, 484.
592 https://doi.org/10.3389/FENVS.2023.1125979

593 Laughner, J. L., & Cohen, R. C. (2019). Direct observation of changing NOx lifetime in North American cities.
594 *Science*, *366*(6466), 723–727. https://doi.org/10.1126/science.aax6832

595 Levelt, P. F., Joiner, J., Tamminen, J., Veefkind, J. P., Bhartia, P. K., Zweers, D. C. S., et al. (2018). The Ozone
596 Monitoring Instrument: Overview of 14 years in space. *Atmospheric Chemistry and Physics*, *18*(8), 5699–
597 5745. https://doi.org/10.5194/acp-18-5699-2018

598 Lin, M., Horowitz, L. W., Hu, L., & Permar, W. (2024). Reactive Nitrogen Partitioning Enhances the Contribution
599 of Canadian Wildfire Plumes to US Ozone Air Quality. *Geophysical Research Letters*, *51*(15).
600 https://doi.org/10.1029/2024GL109369

601 Liu, F., Beirle, S., Zhang, Q., Dörner, S., He, K., & Wagner, T. (2016). NOx lifetimes and emissions of cities and
602 power plants in polluted background estimated by satellite observations. *Atmospheric Chemistry and Physics*,
603 *16*(8), 5283–5298. https://doi.org/10.5194/acp-16-5283-2016

604 Liu, S., Valks, P., Pinardi, G., Xu, J., Chan, K. L., Argyrouli, A., et al. (2021). An improved TROPOMI
605 tropospheric NO2 research product over Europe. *Atmospheric Measurement Techniques*, *14*(11), 7297–7327.
606 https://doi.org/10.5194/amt-14-7297-2021

607 Liu, X., Wang, Y., Wasti, S., Li, W., Soleimanian, E., Flynn, J., et al. (2023). Evaluating WRF-GC v2.0 predictions
608 of boundary layer height and vertical ozone profile during the 2021 TRACER-AQ campaign in Houston,
609 Texas. *Geoscientific Model Development*, *16*(18), 5493–5514. https://doi.org/10.5194/gmd-16-5493-2023

610 Lorente, A., Folkert Boersma, K., Yu, H., Dörner, S., Hilboll, A., Richter, A., et al. (2017). Structural uncertainty in
611 air mass factor calculation for NO2 and HCHO satellite retrievals. *Atmospheric Measurement Techniques*,
612 *10*(3), 759–782. https://doi.org/10.5194/amt-10-759-2017

613 Martin, R. V., Brauer, M., van Donkelaar, A., Shaddick, G., Narain, U., & Dey, S. (2019). No one knows which city
614 has the highest concentration of fine particulate matter. *Atmospheric Environment: X*, 100040.
615 https://doi.org/10.1016/J.AEAOA.2019.100040

616 Maruhashi, J., Mertens, M., Grewe, V., & Dedoussi, I. C. (2024). A multi-method assessment of the regional
617 sensitivities between flight altitude and short-term O3 climate warming from aircraft NOx emissions.
618 *Environmental Research Letters*. https://doi.org/10.1088/1748-9326/ad376a

619 Nault, B. A., Laughner, J. L., Wooldridge, P. J., Crounse, J. D., Dibb, J., Diskin, G., et al. (2017). Lightning NOx
620 Emissions: Reconciling Measured and Modeled Estimates With Updated NOx Chemistry. *Geophysical*
621 *Research Letters*, *44*(18), 9479–9488. https://doi.org/10.1002/2017GL074436

622 Nawaz, M. O., Goldberg, D. L., Kerr, G. H., & Anenberg, S. C. (2025). TROPOMI Satellite Data Reshape NO2 Air
623 Pollution Land-Use Regression Modeling Capabilities in the United States. *ACS ES&T Air*.
624 https://doi.org/10.1021/acsestair.4c00153

625 Palmer, P. I., Jacob, D. J., Chance, K. V., Martin, R. V., Spurr, R. J. D., Kurosu, T. P., et al. (2001). Air mass factor
626 formulation for spectroscopic measurements from satellites: Application to formaldehyde retrievals from the
627 Global Ozone Monitoring Experiment. *Journal of Geophysical Research: Atmospheres*, *106*(D13), 14539–
628 14550. https://doi.org/10.1029/2000JD900772

https://doi.org/10.5194/egusphere-2025-1350
Preprint. Discussion started: 15 April 2025

629 Platt, U. (1994). Differential Optical Absorption Spectroscopy (DOAS). In *Air monitoring by spectroscopic*
630 *techniques* (p. 531). Wiley-IEEE.

631 Rijsdijk, P., Eskes, H., Dingemans, A., Boersma, K. F., Sekiya, T., Miyazaki, K., & Houweling, S. (2025).
632 Quantifying uncertainties in satellite NO2 superobservations for data assimilation and model evaluation.
633 *Geoscientific Model Development*, *18*(2), 483–509. https://doi.org/10.5194/gmd-18-483-2025

634 Ryu, Y. H., Hodzic, A., Barre, J., Descombes, G., & Minnis, P. (2018). Quantifying errors in surface ozone
635 predictions associated with clouds over the CONUS: A WRF-Chem modeling study using satellite cloud
636 retrievals. *Atmospheric Chemistry and Physics*, *18*(10), 7509–7525. https://doi.org/10.5194/acp-18-7509-2018

637 Sarwar, G., Hogrefe, C., Henderson, B. H., Mathur, R., Gilliam, R., Callaghan, A. B., et al. (2024). Impact of
638 particulate nitrate photolysis on air quality over the Northern Hemisphere. *Science of The Total Environment*,
639 *917*, 170406. https://doi.org/10.1016/j.scitotenv.2024.170406

640 Shah, V., Jacob, D. J., Li, K., Silvern, R. F., Zhai, S., Liu, M., et al. (2020). Effect of changing NOx lifetime on the
641 seasonality and long-term trends of satellite-observed tropospheric NO2 columns over China. *Atmospheric*
642 *Chemistry and Physics Discussions*, *20*(3), 1483–1495. https://doi.org/10.5194/acp-2019-670

643 Shah, V., Keller, C. A., Knowland, K. E., Christiansen, A., Hu, L., Wang, H., et al. (2024). Particulate Nitrate
644 Photolysis as a Possible Driver of Rising Tropospheric Ozone. *Geophysical Research Letters*, *51*(5).
645 https://doi.org/10.1029/2023GL107980

646 Shetty, S., Schneider, P., Stebel, K., David Hamer, P., Kylling, A., & Koren Berntsen, T. (2024). Estimating surface
647 NO2 concentrations over Europe using Sentinel-5P TROPOMI observations and Machine Learning. *Remote*
648 *Sensing of Environment*, *312*, 114321. https://doi.org/10.1016/j.rse.2024.114321

649 Sullivan, D. M., & Krupnick, A. (2018). *Using Satellite Data to Fill the Gaps in the US Air Pollution Monitoring*
650 *Network*. NW. Retrieved from www.rff.org

651 Sun, K., Zhu, L., Cady-Pereira, K. E., Chan Miller, C., Chance, K. V., Clarisse, L., et al. (2018). A physics-based
652 approach to oversample multi-satellite, multi-species observations to a common grid. *Atmospheric*
653 *Measurement Techniques Discussions*, *11*(12), 1–30. https://doi.org/10.5194/amt-2018-253

654 Sun, W., Tack, F., Clarisse, L., Schneider, R., Stavrakou, T., & Van Roozendael, M. (2024). Inferring Surface NO2
655 Over Western Europe: A Machine Learning Approach With Uncertainty Quantification. *Journal of*
656 *Geophysical Research: Atmospheres*, *129*(20). https://doi.org/10.1029/2023JD040676

657 Thornton, J. A., Wooldridge, P. J., & Cohen, R. C. (2000). Atmospheric NO2: In Situ Laser-Induced Fluorescence
658 Detection at Parts per Trillion Mixing Ratios. *Analytical Chemistry*, *72*(3), 528–539.
659 https://doi.org/10.1021/ac9908905

660 Vandaele, A. C., Hermans, C., Simon, P. C., Carleer, M., Colin, R., Fally, S., et al. (1998). Measurements of the
661 NO2 absorption cross-section from 42 000 cm−1 to 10 000 cm−1 (238–1000 nm) at 220 K and 294 K. *Journal*
662 *of Quantitative Spectroscopy and Radiative Transfer*, *59*(3–5), 171–184. https://doi.org/10.1016/S0022-
663 4073(97)00168-4

664 Veefkind, J. P., Aben, I., McMullan, K., Förster, H., de Vries, J., Otter, G., et al. (2012). TROPOMI on the ESA
665 Sentinel-5 Precursor: A GMES mission for global observations of the atmospheric composition for climate, air
666 quality and ozone layer applications. *Remote Sensing of Environment*, *120*(2012), 70–83.
667 https://doi.org/10.1016/j.rse.2011.09.027

https://doi.org/10.5194/egusphere-2025-1350
Preprint. Discussion started: 15 April 2025

668 Zare, A., Romer, P. S., Nguyen, T., Keutsch, F. N., Skog, K., & Cohen, R. C. (2018). A comprehensive organic
669 nitrate chemistry: Insights into the lifetime of atmospheric organic nitrates. *Atmospheric Chemistry and*
670 *Physics*, *18*(20), 15419–15436. https://doi.org/10.5194/acp-18-15419-2018

671

672

673